

# 1 **A multi-proxy assessment of terrace formation in the lower Trinity** 2 **River valley, Texas**

3  
4 Hima J. Hassenruck-Gudipati<sup>1</sup>, Thaddeus Ellis<sup>1</sup>, Timothy A. Goudge<sup>1</sup>, David Mohrig<sup>1</sup>

5 <sup>1</sup>Department of Geosciences, Jackson School of Geosciences, The University of Texas at Austin, Austin, 78712, USA

6 *Correspondence to:* Hima J. Hassenruck-Gudipati (himahg@utexas.edu)

7 **Abstract.** A proposed null hypothesis for fluvial terrace formation is that internally generated or autogenic processes such as  
8 lateral migration and river-bend cutoff produce variabilities in channel incision that lead to the abandonment of floodplain  
9 segments as terraces. Alternatively, fluvial terraces have the potential to record past environmental changes from external  
10 forcings that include temporal changes in sea-level and hydroclimate. Terraces in the Trinity River valley have been previously  
11 characterized as Deweyville groups and interpreted to record episodic cut and fill during late Pleistocene sea-level variations.  
12 Our study uses high-resolution topography of a bare-earth digital elevation model derived from airborne lidar surveys along  
13 ~88 linear km of the modern river valley. We measure both differences in terrace elevations and widths of paleo-channels  
14 preserved on these terraces in order to have two independent constraints on terrace formation mechanisms. For 52 distinct  
15 terraces, we quantify whether ~~there is a clustering of~~ terrace elevations ~~fit distinct planes~~ – expected for allogenic terrace  
16 formation tied to punctuated sea-level and/or hydroclimate change – by comparing variability in a grouped set of Deweyville  
17 terrace elevations against variability associated with randomly selected terrace sets. Results show Deweyville groups record  
18 an initial valley floor abandoning driven by allogenic forcing, which transitions into autogenic forcing for the formation of  
19 younger terraces. For these different terrace sets, the slope amongst different terraces stays constant. For 79 paleo-channel  
20 segments preserved on these terraces, we connected observed changes in paleo-channel widths to estimates for river paleo-  
21 hydrology over time. Our measurements suggest the discharge of the Trinity River increased systematically by a factor of ~2  
22 during the late Pleistocene. Despite this evidence of increased discharge, the similar down-valley slopes between terrace sets  
23 indicate that there were likely no increases in sediment-to-water discharge ratios that could be linked to allogenic terrace  
24 formation. This is consistent with our elevation clustering analysis that suggests younger terraces are indistinguishable in their  
25 elevation variance from autogenic terrace formation mechanisms, even if the changing paleo-channel dimensions might,  
26 viewed in isolation, provide a mechanism for allogenic terrace formation. Methods introduced here combine river-reach scale  
27 observations of terrace sets and paleohydrology with local observations of terraces and paleo-channels to show how  
28 interpretations of allogenic versus autogenic terrace formation can be evaluated within a single river system.

## 29 1 Introduction

30 River valleys commonly contain fluvial terraces representing segments of older floodplain that are now located at  
31 elevations distinctly above the modern floodplain. These terraces sometimes preserve paleo-channels, or remnant river-channel  
32 segments. For exceptionally preserved features, channel widths, depths, bend amplitudes and wavelengths, and grain size  
33 record a signal of past river hydrology. Terrace formation requires net river incision that can be allogenicly driven by tectonic  
34 uplift, sea-level fall, and/or modifications to water and sediment discharge via climate change or land-use change, including  
35 dam construction (Bull, 1990; Hancock and Anderson, 2002; Mackey et al., 2011; Pazzaglia, 2013; Womack and Schumm,  
36 1977). What is more controversial is the character of the trigger that leads to the relatively discrete transfer of a section of  
37 active floodplain or valley floor into an inactive terrace or set of terraces elevated above flood height. In particular, can terraces  
38 formed by a punctuated sea-level fall, tectonic uplift, or sediment-to-water flux change be accurately separated from terraces  
39 formed by lateral migration and incision connected with the autogenic processes of river channel migration and channel-bend  
40 cutoff? Here we use attributes of terraces and their preserved paleo-channels in the coastal Trinity River valley in order to  
41 evaluate the likelihood of allogenic versus autogenic triggers driving terrace formation for previously established groups of  
42 Deweyville terraces (Bernard, 1950; Blum et al., 1995). Understanding how these terraces were most likely formed will help  
43 to constrain interpretations of the input signals for downstream deltaic deposits, which are recognized to embed both allogenic  
44 and autogenic signals (Guerit et al., 2020).

45 Commonly invoked allogenic triggers connected with terrace formation are (1) punctuated decreases in sediment-to-  
46 water flux that are assumed to embed a signal of regional climate change and (2) punctuated base-level fall controlled by either  
47 sea-level fall or tectonic uplift, all of which can drive periods of increased vertical incision along an extended length of river  
48 channel (Blum et al., 1995; Blum and Törnqvist, 2000; Bull, 1990; Daley and Cohen, 2018; Hancock and Anderson, 2002;  
49 Merritts et al., 1994; Pazzaglia, 2013; Pazzaglia and Gardner, 1993; Rodriguez et al., 2005; Wegmann and Pazzaglia, 2002).  
50 These focused periods of downcutting are interpreted to produce a spatially extensive terrace, or set of terraces, that preserve  
51 a fraction of the active fluvial surface and its river channel at the time of the terrace-forming event (Bull, 1990; Molnar et al.,  
52 1994; Pazzaglia, 2013; Pazzaglia et al., 1998). One expected morphology for terraces formed by allogenic triggers are extensive  
53 terraces flanking both sides of the river at a similar elevation, which would be expected during synchronous river incision.  
54 However, it is important to realize that the extent and pairing of these terraces can be substantially modified during ongoing  
55 valley incision and that unequal channel migration during relatively slow incision rates can produce similar characteristics  
56 (Limaye and Lamb, 2016; Malatesta et al., 2017).

57 Both theory (Parker et al., 1998a; Wickert and Schildgen, 2019) and experiments (Tofelde et al., 2019; Whipple et  
58 al., 1998) have shown how the long profile of a fluvial valley is set by the ratio of sediment-to-water discharge. Decreases in  
59 water-to-sediment flux led to slope increases via alluviation. Conversely, increases in water-to-sediment flux produce lower  
60 slopes through channel incision and valley formation. An allogenic trigger for terrace formation associated with  
61 paleohydrology change is therefore expected to produce a long profile for older terraces that are steeper than the long profile

62 of the younger and incising river. This reduction ~~from the measured in paleo-~~slopes ~~from older~~of terrace sets to the modern  
63 ~~channel-floodplain~~ has been observed in both natural (Poisson and Avouas, 2004) and experimental (Tofelde et al., 2019)  
64 systems. Interestingly, a change in climate that produced similar decreases or increases in both the water and sediment  
65 discharges would yield no change in the downstream slope of the system and no episode of incision to drive terrace formation.  
66 Since water and sediment discharges are strongly correlated within fluvial systems (Blom et al., 2017; Lane, 1955), it is quite  
67 possible that climate change might not provide an allogenic trigger for terrace formation. If long profiles extracted from terrace  
68 sets are parallel to the slope of the modern river than a different driver of incision must be at work. In the greater coastal zone  
69 this can be a base-level drop tied to sea-level fall (Tofelde et al., 2019). For this reason it is tempting to use interpreted sets of  
70 subparallel terraces as a proxy record for fluctuations in sea-level through time (Blum et al., 1995; Blum and Törnqvist, 2000;  
71 Merritts et al., 1994; Rodriguez et al., 2005).

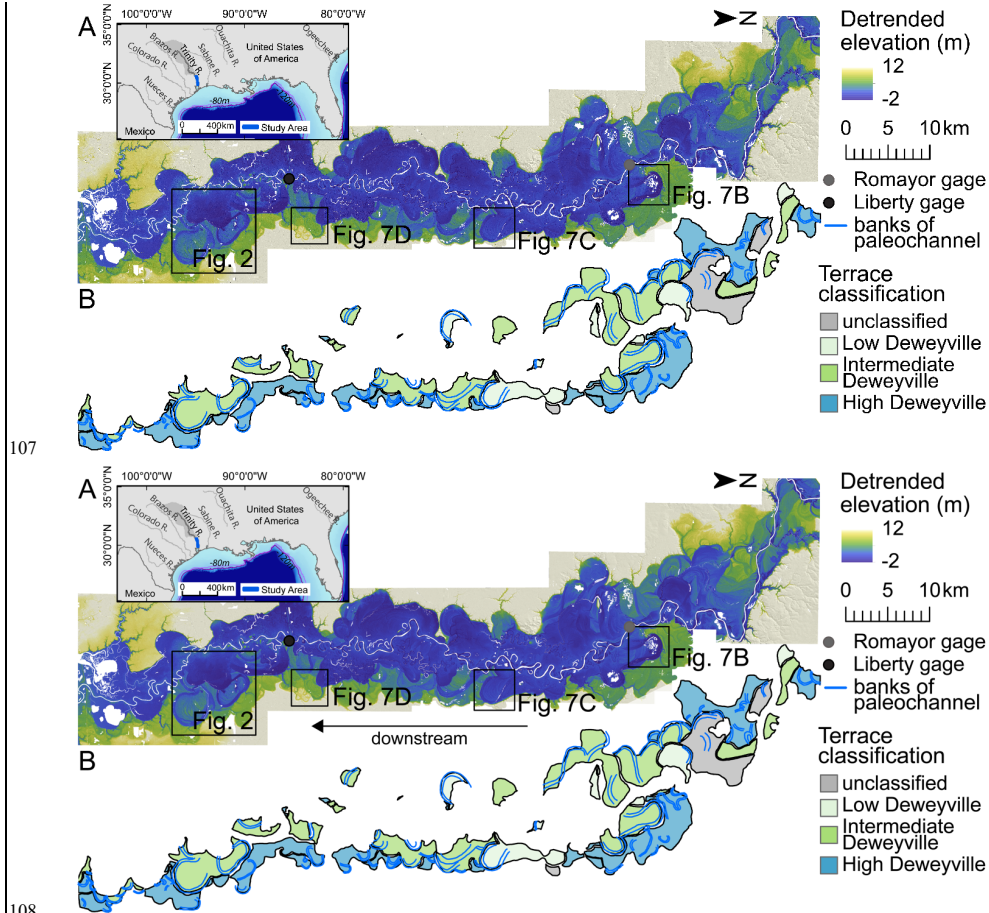
72 It has also been shown that terraces can form by autogenic processes that drive spatially variable incision rates under  
73 conditions of persistent, allogenic forced base-level fall (Bull, 1990; Finnegan and Dietrich, 2011; Limaye and Lamb,  
74 2014; Merritts et al., 1994; Muto and Steel, 2004; Strong and Paola, 2006). Autogenic terraces can be produced by channel  
75 narrowing (Lewin and Macklin, 2003; Muto and Steel, 2004; Strong and Paola, 2006) and river-bend cut off (Erkens et al.,  
76 2009), both of which can increase bed incision rates via upstream propagating knickpoints (Finnegan and Dietrich, 2011).  
77 Processes that lead to terraces that have autogenic characteristics include local variations in channel dynamics, ~~bedrock-channel~~  
78 ~~bed~~ slope, and sediment contribution from tributaries (Erkens et al., 2009; Lewin and Macklin, 2003; Womack and Schumm,  
79 1977). In particular, river bend cut-off can locally increase the channel slope, driving channel-bed incision that transitions a  
80 segment of floodplain into a terrace (Erkens et al., 2009; Finnegan and Dietrich, 2011). This autogenic trigger produces terrace  
81 heights consistent with elevation drops associated with bend cutoffs (Finnegan and Dietrich, 2011). An additional autogenic  
82 process that can trigger terrace formation is variable rates of lateral channel migration during persistent base-level fall (Lewin  
83 and Macklin, 2003; Limaye and Lamb, 2016). Both unsteady lateral migration and bend cut-off preferentially generate terraces  
84 that host only a small number of paleo-channel bends (Finnegan and Dietrich, 2011).

85 Here we present a study of three previously classified sets of fluvial terraces composing the Deweyville ~~Allogroup~~  
86 ~~allostratigraphic units~~ of the lower Trinity River valley that have previously been described occurring at three distinct elevation  
87 trends (Bernard, 1950; Blum et al., 1995; Heinrich et al., 2020; Young et al., 2012). These terraces have been interpreted as  
88 forming in response to allogenic triggers that include Pleistocene sea-level fluctuations and climate-controlled changes in  
89 water-to-sediment discharge (Anderson et al., 2016; Blum et al., 2013, 1995; Blum and Aslan, 2006; Rodriguez et al., 2005;  
90 Saucier and Fleetwood, 1970). We analyze whether these purported allogenic triggers can be distinguished from a null  
91 hypothesis that terraces were formed by autogenic processes during long-term valley incision associated with persistent sea-  
92 level fall during the Last Glacial Period (from the end of the Eemian to the Last Glacial Maximum). To do this we implement  
93 a multi-proxy approach that (1) compares variability in terrace elevations for each classified set against elevation variability  
94 for randomly selected terraces, (2) evaluates temporal changes in paleo-hydrology as defined by segments of paleo-channels  
95 preserved on terrace surfaces, and (3) relates paleo-slopes defined by the terrace sets to the long profile of the modern Trinity

96 River. Our analysis reveals that the upper set of terraces is most likely the product of an allogenic trigger, while the lowest set  
97 of terraces is most likely the product of autogenic processes. The formational driver for the third, intermediate set of terraces  
98 is equivocal. This result documents how the study of terraces can be employed to substantially refine paleo-environmental  
99 interpretations that are generated using these preserved fragments of relict landscapes.

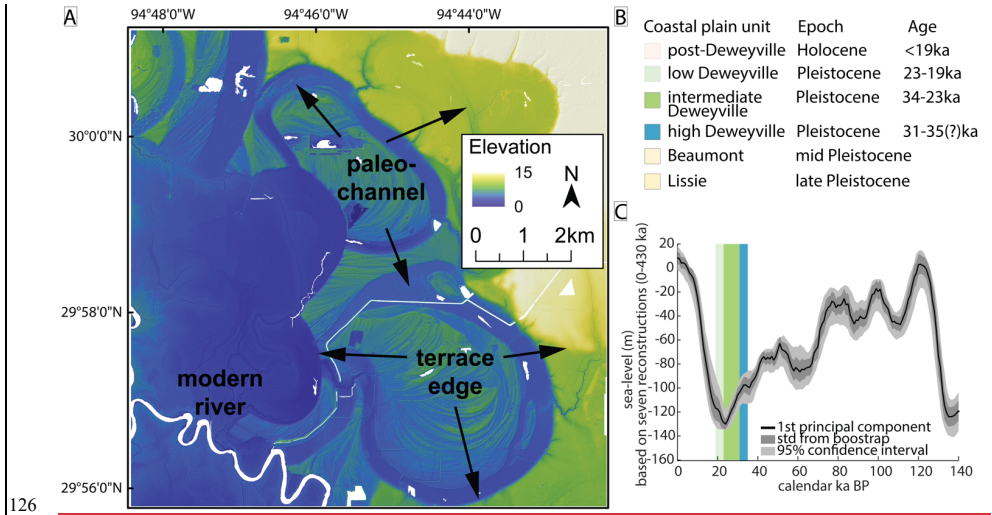
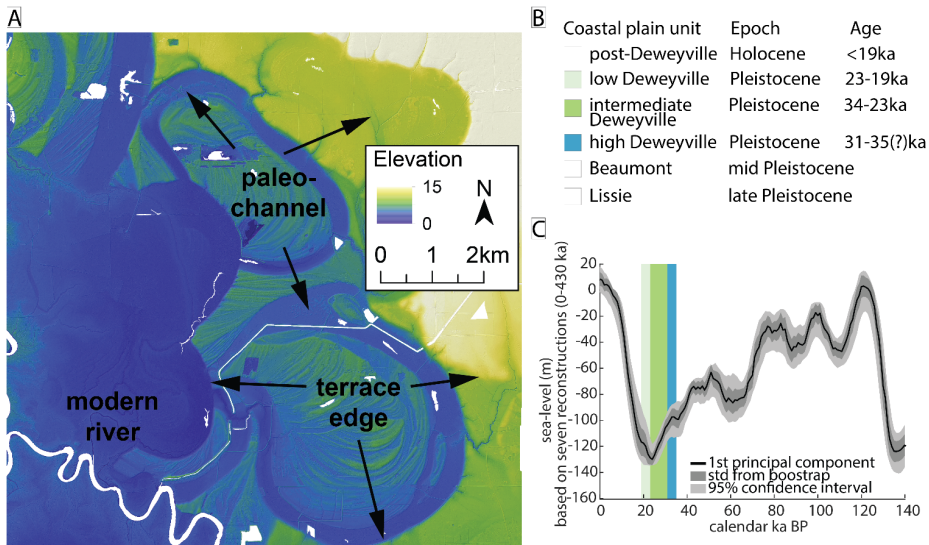
## 100 **2 Geological Setting**

101 The Trinity River has the largest drainage basin contained entirely within the state of Texas, with an area of over  
102 46,000 km<sup>2</sup>. It flows from northwest of Dallas, Texas, to Trinity Bay, where it empties into the Gulf of Mexico. Our study area  
103 is an ~88 linear-km stretch of the lowermost Trinity River valley from just north of Romayor, Texas, to just north of Wallisville,  
104 Texas (**Fig. 1**). Prone to flooding, the Trinity River has a median peak-annual discharge of 1679 m<sup>3</sup>/s at Romayor, TX (USGS  
105 08066500) and 1484 m<sup>3</sup>/s at Liberty, TX (USGS 08067000) for the 2000 – 2020 hydrograph (U.S. Geological Survey, 2020a,  
106 2020b).



109 Figure 1. (A) 2011 bare earth digital elevation model (DEM) from airborne lidar with (B) terrace and paleo-channel outlines of the  
 110 Trinity River, Texas, valley. (A) The lidar DEM has been detrended using the modern valley slope to emphasize local elevation  
 111 variability. The black boxes mark the extent of Fig. 2 and 7B-D. USGS gage stations at Romayor and Liberty are marked in grey  
 112 and black, respectively. The downstream extent of the data is ~10 linear km upstream of the river outlet into the Trinity Bay of the  
 113 Galveston Bay. (B) Terraces are preferentially distributed on the east of the valley.

114 The Trinity River has been subject to climate and sea-level variations throughout the Quaternary (Anderson et al.,  
115 2014; Galloway et al., 2000; Simms et al., 2007); however, the river catchment has never been glaciated and is interpreted to  
116 have maintained an approximately constant drainage area over this time (Hidy et al., 2014). The lower Trinity River valley is  
117 incised into the Beaumont and Lissie formations of Middle to Late Pleistocene age (Baker, 1995). Within the valley,  
118 Deweyville ~~Allogroup~~-terraces are post-Beaumont in age and formed prior to the Holocene (**Fig. 2A-B**). Age equivalent  
119 terraces with preserved segments of large paleo-channels are also found in alluvial valleys ranging from Mexico to South  
120 Carolina and are often classified as belonging to the same Deweyville ~~Allogroup~~bounding surface and allostratigraphic unit.  
121 Traditionally, the formation of Deweyville terraces has been interpreted as the product of high frequency Pleistocene sea-level  
122 cycles (Anderson et al., 2016; Bernard, 1950; Blum et al., 1995) with distinct episodes of incision and subsequent valley  
123 deposition (Blum et al., 2013; Blum and Aslan, 2006). The history of climatic variation, lack of glaciation, and superb  
124 preservation of late Pleistocene terraces make the lower Trinity River valley an ideal location to study terrace formation and  
125 to ask what processes these geomorphic features record.



127  
128 **Figure 2. (A) Morphological features of the Trinity River valley. Several terraces are preserved at different elevations with the black**  
129 **arrows marking the edges of the terraces. The labelled paleo-channel has a width that is ~2 times the modern river channel width.**  
130 **(B) Regional stratigraphic framework (Garvin, 2008; Blum et al., 2013). (C) Global sea-level from seven reconstructions based on**  
131 **(Spratt and Lisiecki, 2016) and Deweyville Allogroup terrace ages from (B) range in (light green, green, and blue).**

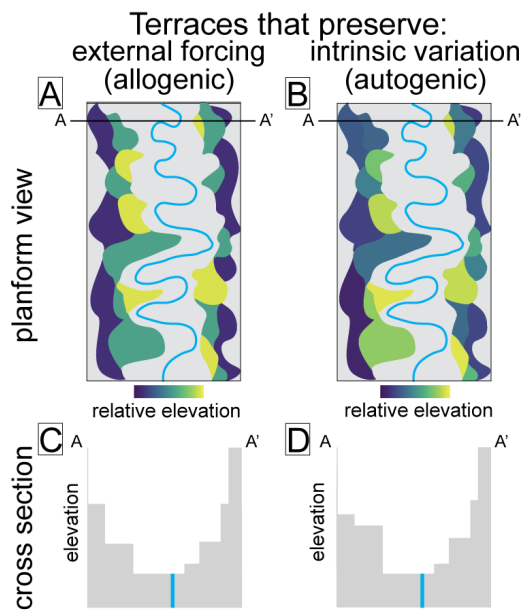
132 The Deweyville terraces ~~are associated with bounding surfaces of have been divided into~~ three  
133 ~~Allogroups~~allostratigraphic units, and can be grouped into three sets of terraces: high, intermediate, and low (Bernard, 1950;  
134 Blum et al., 1995; Young et al., 2012). Sea-level rise during the Holocene has induced valley-floor sedimentation that has  
135 partially buried the low-terrace ~~Allogroup~~bounding surface (Blum et al., 1995; Blum and Aslan, 2006). Age control for  
136 terraces in the lower Trinity River valley is limited to eight dates using optically stimulated luminescence (OSL) (Garvin,  
137 2008). Based on these data, Garvin (2008) reports an OSL age of 35 - 31 ka for channel activity on high Deweyville terraces  
138 (N = 1), 34 - 23 ka for intermediate Deweyville terraces (N = 4), and 23 - 19 ka for low Deweyville terraces (N = 3). With  
139 only a single OSL date from the high Deweyville terraces, these features could be as old as 60-65 ka based on existing  
140 stratigraphic frameworks (Blum et al., 2013).

141 The global sea-level curve shows an overall range of ~33m between 35 and 19ka (Fig. 2C, Spratt and Lisiecki, 2016).  
142 The Pleistocene sea-level curve for the Gulf of Mexico during the period of Deweyville terrace formation shows high-  
143 frequency variability superimposed on a longer-term net sea-level fall (Anderson et al., 2016; Simms et al., 2007). Between  
144 35 and 19 ka, short-term rises and falls in sea-level are estimated to have been as large as 20 m and 60 m, respectively  
145 (Anderson et al., 2016). Deweyville ~~Allogroups~~bounding surfaces have been interpreted to represent three discrete sets of  
146 terraces formed during distinct oscillations in sea-level (Anderson et al., 2016; Bernard, 1950; Blum et al., 1995; Morton et  
147 al., 1996; Rodriguez et al., 2005; Thomas and Anderson, 1994). The three sets of terraces also have been interpreted as  
148 recording episodes of relative sea-level stasis with extensive lateral migration of the river channel, separated by punctuated  
149 incision tied to accelerated sea-level fall (Blum et al., 2013; Blum and Aslan, 2006). The commonality between these two  
150 interpretations is an allogenic driver for terrace formation.

151 Paleo-channels have long been recognized to record past hydrologic conditions and associated climatic variations  
152 (Church, 2006; Knox, 1985). Terraces of the Trinity River valley preserve segments of abandoned river channels that range in  
153 apparent widths and depths (Fig. 2). Previous researchers have interpreted increases in these paleo-channel widths and radii-  
154 of-curvature for paleo-channel bends as products of increases in river discharge and precipitation (Church, 2006; Knox, 1985;  
155 Saucier and Fleetwood, 1970; Sylvia and Galloway, 2006), and possible associated changes in vegetation and/or bank  
156 erodibility (Alford and Holmes, 1985; Blum et al., 1995; Saucier, 1994). Paleo-channel morphologies thus provide a record of  
157 external paleo-environmental change in the lower Trinity River valley that is independent of any signal encapsulated in terrace  
158 formation. Therefore, using both terrace elevations and paleo-channels, we have two geomorphic proxies to compare and  
159 contrast while assessing terrace formational processes among the Deweyville ~~Allogroups~~bounding surfaces.

160 **3 Null Hypothesis: Terrace Formation**

161 Following the proposal of Limaye and Lamb (2016), our null hypothesis for terrace formation is that punctuated  
162 incision by autogenic triggers dominate terrace development. Only after formational mechanisms internal to the system have  
163 been considered and rejected, should we consider allogenic triggers for terrace formation. Our method for testing the null  
164 hypothesis acts to separate the regional expression of an allogenic driver from more localized terrace production by autogenic  
165 processes. It is based on the observation that allogenic triggers produce synchronous, regionally extensive terraces that  
166 approximately preserve surface elevations defining a single paleo-valley slope (Bull, 1990; Pazzaglia et al., 1998). It therefore  
167 follows that a group of terraces formed by a contemporaneous allogenic trigger should preserve lower variability in elevations  
168 about a best-fit plane estimating this paleo-slope than groupings of randomly selected terraces (Fig. XA). Conversely,  
169 autogenically produced terraces preserve a multitude of elevations that we do not expect to define a contemporaneous long  
170 profile (Fig. XB). Therefore, groupings of local autogenic terraces are expected to be indistinguishable from sets composed of  
171 randomly selected terraces.



172

173 ~~Figure 3. Conceptual diagram showing distribution of terrace elevations expected in planform view (A-B) and cross sectional view~~  
174 ~~(C-D) for allogenic triggers (A, C) and autogenic triggers that form terraces (B, D). Here we show three distinct terrace sets for~~  
175 ~~autogenic triggers and an undistinguishable number of terrace sets.~~

#### 176 4 Approaches and Observations

177 Our study used elevation data derived from four airborne lidar surveys collected for the Federal Emergency  
178 Management Agency (FEMA) and Texas' Strategic Mapping Program (StartMap) in 2011, 2017, and 2018 (FEMA, 2011;  
179 StartMap, 2017a; StartMap, 2017b; StartMap, 2018). These four surveys were merged to produce a single bare earth digital  
180 elevation model (DEM) with a 1 m grid spacing. The horizontal accuracies of the four original lidar point clouds from 2011,  
181 2017a, 2017b, and 2018 are 0.6 m and 0.4 m, 0.25 m and 0.29 m, 0.20 m and 0.20 m, and 0.20 m and 0.20 m, respectively. All  
182 data were referenced to the NAD83 horizontal datum. The vertical accuracy for the original lidar point clouds from 2011,  
183 2017a, 2017b, and 2018 are 0.4m, 0.29m, 0.20m, and 0.20m, respectively, and all data were referenced to the NAVD88 vertical  
184 datum.

185 Individual terraces and paleo-channels were manually mapped on the merged DEM using ArcGIS. A terrace was  
186 defined as a genetically similar surface that is offset in elevation from its surrounding topography. Previously, Blum et al.  
187 (1995) mapped terraces on the Trinity River, which was extended by Garvin (2008), using a combination of satellite images  
188 and DEMs. Based on these maps, terraces were classified as high, intermediate, or low Deweyville or marked as unclassified  
189 if the surface had not been previously identified in Garvin (2008). Care was taken to only map the sections of terrace surfaces  
190 that did not appear to be modified by later fluvial processes. Elevations defining each terrace were extracted from the DEM  
191 using a 5 m grid resolution for a total of 164,520 measurements across all mapped terraces. A grid resolution lower than the  
192 DEM resolution was selected to conserve available computational resources and to speed up analyses. Mapping on the 5-m  
193 grid still produced hundreds of points for bare-earth elevation on each terrace, thereby producing estimates for the topography  
194 that are comparable to calculations made using the full resolution DEM.

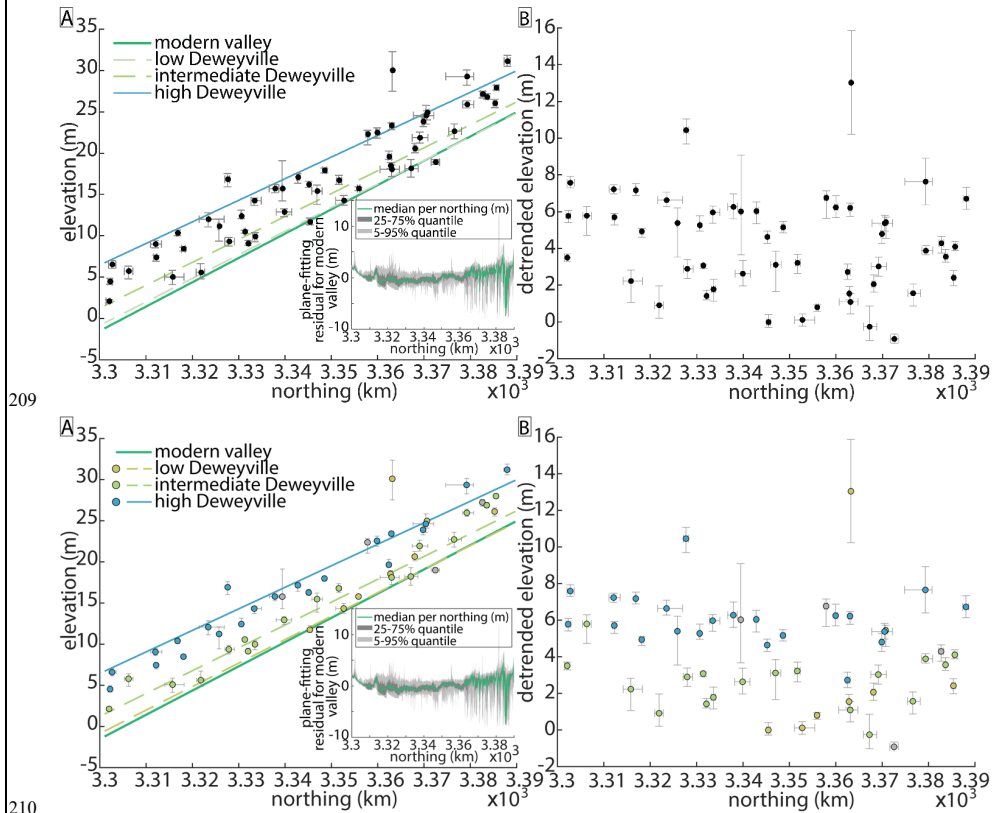
195 From these elevations, the median value and interquartile range were found for each ~~of the 52 mapped terraces~~. Since  
196 the Trinity River valley in the study area trends N-S, the elevation data for each terrace is plotted against median UTM northing  
197 in ~~Fig. 3A4A. The plane best-fit plane for the modern valley was used to generate detrended elevations for each terrace DEM~~  
198 ~~measurement by subtracting it from the spatially corresponding modern valley best-fit plane value. A best-fit~~This plane  
199 defining the modern valley floor was generated from a subsampled DEM with a 10 m grid resolution. The RMSE of the plane  
200 fit is 1.36 m with most of the >4,500,000 points falling within 5m of the plane. Plotting the residuals to the best-fit plane along  
201 UTM northing reveals some structure in the most downstream southern long profile extent (~~Fig. 3A-4A insert~~), ~~likely due to~~  
202 ~~Holocene sedimentation (Blum et al., 1995; Blum and Aslan, 2006)~~. However, we do not think this affects our detrended  
203 terrace analysis. ~~The plane fit for the modern valley was used to generate detrended elevations for each terrace DEM~~  
204 ~~measurement by subtracting it from the spatially corresponding modern valley best-fit plane value.~~The detrended median

Formatted: Font: 9 pt, Bold

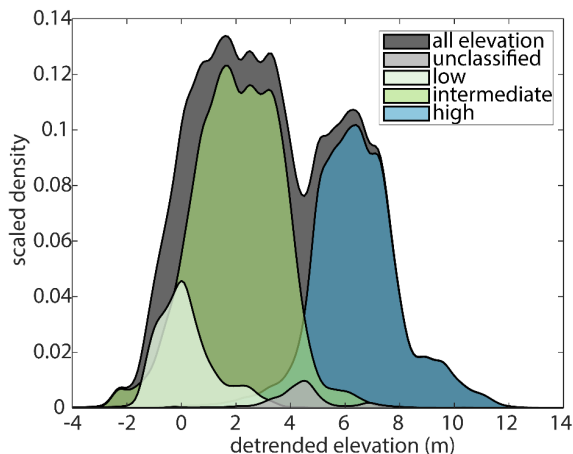
Formatted: Indent: First line: 0"

Formatted: Font: 9 pt, Bold

205 elevations and associated interquartile ranges for each terrace are presented in [Fig. 3B4B](#). We then compared the distributions  
 206 of detrended elevations for the terrace classifications. Each classified distribution, scaled to its contribution to the overall  
 207 number of detrended elevations, is plotted in [Fig. 45](#). Even though their median values are different, the detrended elevation  
 208 distribution for the intermediate Deweyville terraces fully overlaps with that of the low Deweyville terraces ([Fig. 45](#)).



211 **Figure 4-3-** (A) Median terrace elevation and (B) detrended elevation for the 52 terraces along the N-S trending valley, **colored by**  
 212 **terrace category by Blum (1995) and Garvin (2008) as high, intermediate, and low Deweyville. Terraces not previously identify were**  
 213 **left grey.** The error bars represent the interquartile range around the median terrace UTM and elevation values. The dark green  
 214 line corresponds to the plane fitted to the 10m DEM of modern valley elevations and the insert shows the residual of this plane fit.  
 215 Blue, green, and light green lines indicate the plane fit to 1m DEM terrace elevations assigned to each **Deweyville** terrace category  
 216 **by Blum (1995) and Garvin (2008) as high, intermediate, and low Deweyville.**



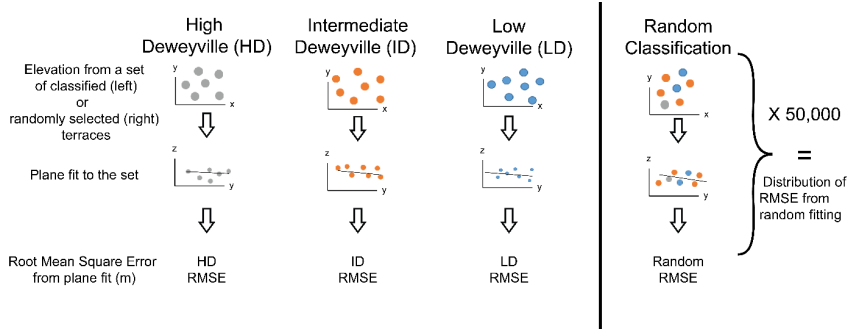
217  
 218 **Figure 45.** Distributions of detrended elevations for terraces classified by Garvin (2008). Distributions were generated using a  
 219 Gaussian kernel with bandwidth = 0.2 and scaled by the proportion of the total elevation points (164,520) present in each  
 220 classification. There are 16,543, 84,784, 60,244, and 2960 points in the low, intermediate, high, and unclassified groupings,  
 221 respectively. There is complete overlap between the detrended elevations of low and intermediate terraces. Terraces classified as  
 222 high and intermediate have less overlap. The median detrended elevations for the low, intermediate, high, and unclassified  
 223 Deweyville groupings are 0.3m, 2.05 m, 6.3 m, and 4.41 m.

224

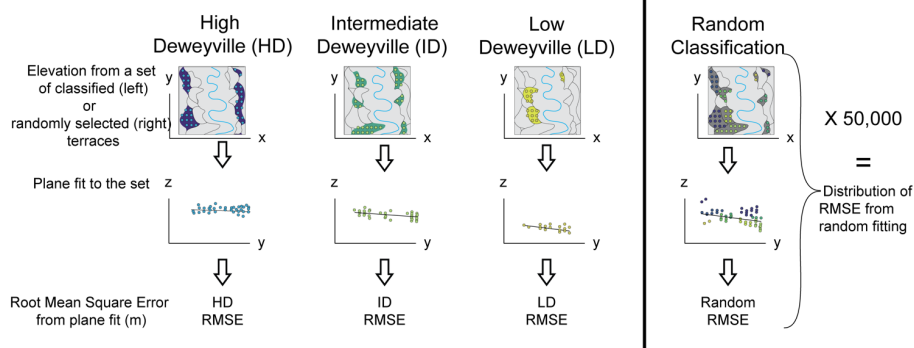
#### 225 4.1 Testing Terrace Formation using Elevation Data

226 We began our hypothesis testing by determining the best-fit plane to all of the [raw](#) elevation points (x, y, z) for terraces  
 227 classified into the three Deweyville groups by Blum et al. (1995) and Garvin (2008) using a linear least-squares method. A  
 228 planar surface was chosen for this analysis because the modern river-surface and valley profiles are near linear in our area of  
 229 study ([Fig. 3A4A](#)). The goodness of fit for these three planes to their associated terrace data was captured by the root-mean-  
 230 square error (RMSE), which provides a measure of average variability of actual terrace elevations about the best-fit plane ([Fig.](#)  
 231 [5-6](#)). The next step was to compare the properties of these fitted planes against planes fit to terraces randomly drawn from the  
 232 overall population. The randomly assigned terraces were put into one of three groups that had the same number of elements as  
 233 the classified high (n=22), middle (n=19), and low (n=8) Deweyville terraces. Best-fit planes were calculated and their RMSE  
 234 was recorded. This process of randomly assigning terraces into three groups was then repeated 50,000 times in order to derive  
 235 a large dataset of elevation variability characterizing randomly grouped terraces ([Fig. 6-7](#))

236

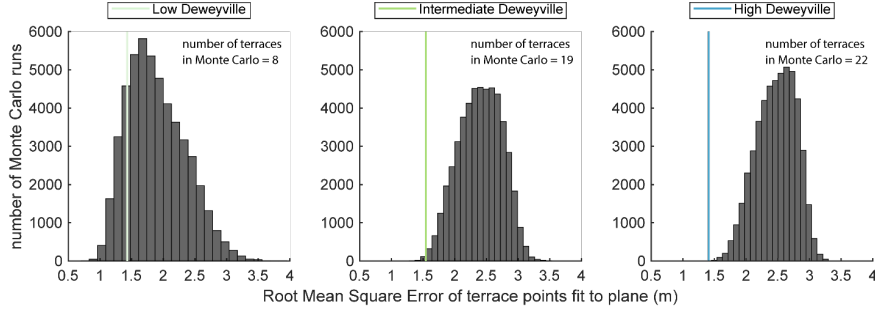


237



238 **Figure S6.** Method to determine if classifications assigned to terraces represent distinct terrace groups. (Left) A plane was first fit to  
 239 elevations extracted from the classified terrace groups in Garvin (2008) at a 5 m grid resolution. (Right) We then fit planes to three  
 240 randomly grouped sets of terraces using the same elevation data, iterating 50,000 times, for a total of 150,000 fits (right of the black  
 241 line). The root mean square error (RMSE) of the plane fit from each of the previously classified terrace groups was compared to the  
 242 distribution of RMSE of the randomly grouped terraces (Fig. 67).

243



244  
 245 **Figure 76.** Root mean square error (RMSE) of a plane fit to elevation points of terraces previously classified as high Deweyville,  
 246 intermediate Deweyville, and low Deweyville in the Trinity River valley compared to a distribution of RMSE from 150,000 randomly  
 247 grouped terraces. **The low, intermediate, and high Deweyville terrace sets have RMSEs of 1.43m, 1.54m, and 1.41m, respectively.**  
 248 All of the Deweyville classifications (light green, green, and blue lines) have an RMSE that falls within the distribution of RMSE for  
 249 randomly grouped terraces. The high Deweyville classification is the closest to falling outside of the distribution, ~3.4 standard  
 250 deviations away from the random terraces RMSE distribution mean of 2.47 m (22 terrace groupings). The low and intermediate  
 251 Deweyville classification are ~1.0 and ~2.5 standard deviations away from the RMSE distribution mean of 1.89 m and 2.40 m for 8  
 252 and 19 terrace groupings, respectively.

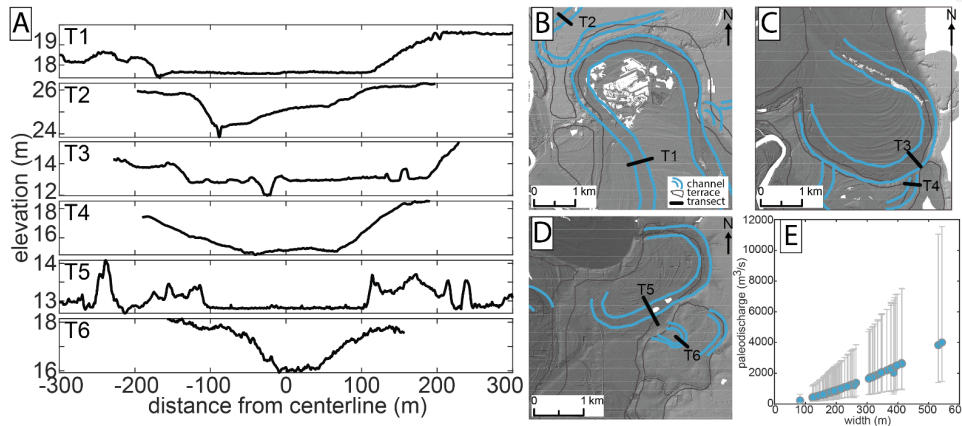
## 253 4.2 Evaluating Terrace Formation using Paleo-Channel Analysis

254 Change in the discharge of the Trinity River during the late Pleistocene was estimated using the 79 mapped segments  
 255 of paleo-channels preserved on terrace surfaces. Mean bankfull width ( $B_{bf}$ ) for each paleo-channel mapped on the bare-earth  
 256 DEM (**Fig. 1B**) was calculated from measurements extracted at 10 m intervals along each paleo-channel centerline (**Fig. 87**).  
 257 Representative sidewall slopes (rise/run) for these paleo-channels range between 0.02 and 0.26 (**Fig. 87A**). These paleo-  
 258 sidewall slopes fall within the range of modern sidewall slopes measured for the Trinity River in the study area by Smith and  
 259 Mohrig, (2017, their Fig. 45). Therefore, we confidently use the paleo-channel widths extracted from the DEM without any  
 260 correction to the widths associated with relaxation of the paleo-topography over time. These data were used to estimate a  
 261 formative, bankfull discharge ( $Q_{bf}$ ) for sand-bed rivers following the hydraulic geometry relationship developed by Wilkerson  
 262 and Parker, (2011):

$$263 \quad \frac{B_{bf} * g^{\frac{1}{2}}}{Q_{bf}^{\frac{2}{5}}} = 0.0398 * \left( \frac{D_{50} * \sqrt{R * g + D_{50}}}{\nu} \right)^{0.494 \pm 0.14} * \left( \frac{Q_{bf}}{D_{50}^2 * \sqrt{g * D_{50}}} \right)^{0.269 \pm 0.031}, \quad (1)$$

264 where  $\nu$  is the kinematic viscosity of water,  $R$  is the specific gravity of the sediment ( $R = \frac{\rho_s - \rho}{\rho}$ ),  $\rho_s$  is sediment density,  $\rho$  is  
 265 water density,  $g$  is gravitational acceleration, and  $D_{50}$  is the median grain size of transported bed material. We used a value of  
 266 2650 kg/m<sup>3</sup> for  $\rho_s$  and a range of paleo-channel grain sizes taken from Garvin (2008), who sampled both the lower and upper  
 267 portions of bar deposits within preserved channel fills (**Table 1**). The uncertainty in estimated discharge was quantified for  
 268 each paleo-channel using Monte Carlo simulation. For each run of the simulation, we sampled from: (1) normal distributions  
 269 with the reported means and standard deviations for each exponent in **Eq. 1**; (2) a normal distribution for channel width using

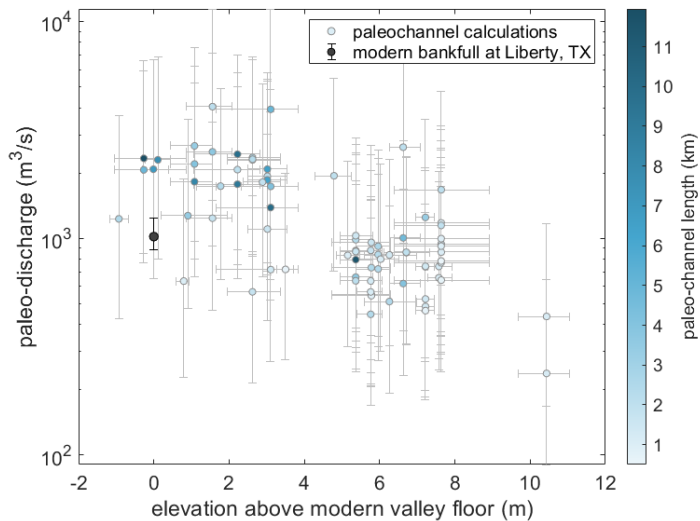
270 its measured mean and standard deviation; and (3) a uniform distribution of grain sizes constrained by measurements from  
 271 each classified terrace set (**Table 1**). This Monte Carlo simulation was run 50,000 times for each paleo-channel. Paleo-  
 272 discharge estimates derived for the 79 channel segments preserved on terrace surfaces are plotted as a function of median  
 273 detrended terrace elevation in **Fig. 98**.



274  
 275 **Figure 87.** Paleo-channel widths and paleo-discharge estimates. (A) Elevation transects for six paleo-channels (T1-T6). Transects  
 276 are taken from locations indicated in (B)-(D) with mapped paleo-channels outlined in blue and terrace extents mapped outlined in  
 277 grey. (E) Paleo-discharge estimates for the Trinity River are plotted as a function of their width. Each paleo-discharge was calculate  
 278 using preserved channel width measurements and the discharge-width relationship from Wilkerson and Parker (2011) (Eq. 1). Error  
 279 bars represent the first and third quartile of paleo-channel discharge estimates.

Garvin (2008) Terrace classification	Upper bar deposit lower range (mm)	Upper bar deposit upper range (mm)	Lower bar deposit lower range (mm)	Lower bar deposit upper range (mm)	Average grain size (mm)
Low Deweyville	0.25	1.00	0.25	4.00	0.71
Middle Deweyville	0.125	1.00	0.50	2.00	0.59
High Deweyville	0.125	2.00	0.25	2.00	0.59

280 **Table 1:** Grain size of terrace deposits from Garvin (2008), used for discharge calculations. The average grain size was calculated  
 281 using the phi (logarithmic) scale.



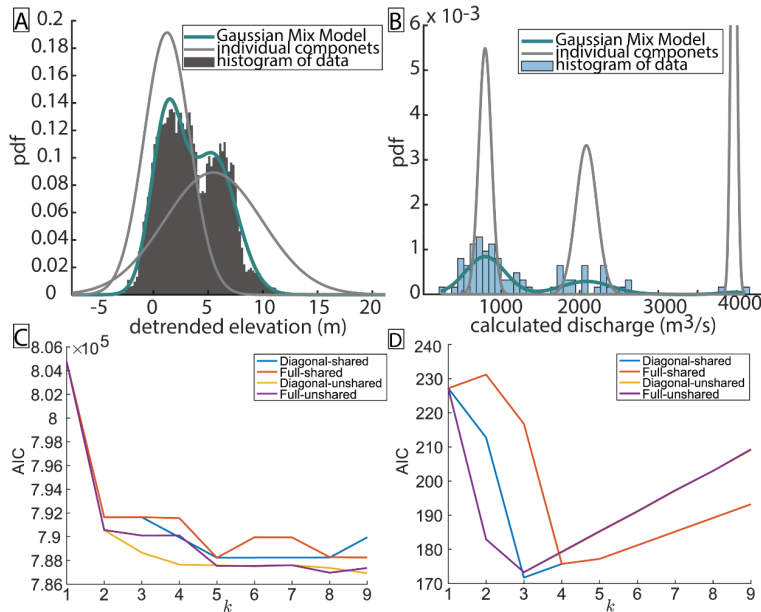
282  
 283 **Figure 98.** Paleo-discharge estimates for the Trinity River plotted as a function of their associated detrended terrace elevations.  
 284 Detrended elevations afford a crude stratigraphy for the discharges with the highest relative elevations representing older channels  
 285 and lowest elevations representing younger channels. Each paleo-discharge was calculated using preserved channel width  
 286 measurements and the discharge-width relationship from Wilkerson and Parker (2011) (Eq. 1). Error bars represent the first and  
 287 third quartile of paleo-channel discharge estimates and terrace elevations above the modern valley. The symbol was shaded to the  
 288 preserved length for each paleo-channel, with darker symbols equated to longer segments. The modern bankfull discharge at  
 289 Liberty, TX was found using the methods described in the text, and plotted at 0m.

290 Accuracy of the Wilkerson and Parker (2011) relationship for the Trinity River system was tested by calculating a  $Q_{bf}$  value  
 291 for the modern river channel and comparing it against the bankfull discharge logged at the USGS gage 08067000 at Liberty,  
 292 Texas. The calculated bankfull discharge was estimated using the measured bankfull width of 170 m from the DEM at the  
 293 gage site. The median particle size of bed material at Liberty has been measured at 200 $\mu$ m by the Trinity River Authority of  
 294 Texas (Trinity River Authority of Texas, 2017). All other variables in Eq. 1 were kept constant between the modern river and  
 295 paleo-channels, yielding an estimate for the modern bankfull discharge of 830 m<sup>3</sup>/s. The reported residual standard error  
 296 associated with the bankfull discharge Eq. 1 (Wilkerson and Parker, 2011) was then used to approximate the error associated  
 297 with this modern calculated bankfull discharge. The lower and upper standard error define a possible range between 340 and  
 298 2030 m<sup>3</sup>/s. These discharges estimated with Eq. 1 compare favorably with the measured discharge found using the rating curve  
 299 for the USGS Liberty gage station ([https://waterdata.usgs.gov/nwisweb/get\\_ratings?file\\_type=exsa&site\\_no=08067000](https://waterdata.usgs.gov/nwisweb/get_ratings?file_type=exsa&site_no=08067000)) and  
 300 bank-line elevations for the swath of channel extending 300 m both upstream and downstream of the gage. The mean and

301 standard deviation of bank elevations for this swath was 7.68m and 0.34m, yielding a mean bankfull discharge of 1017 m<sup>3</sup>/s  
 302 and discharges of 887 m<sup>3</sup>/s and 1243 m<sup>3</sup>/s corresponding to stages  $\pm 1$  standard deviation in bank elevation.

### 303 4.3 Mixing Models and Bend Cutoff Analyses

304 To test the existence of statistical groupings within our terrace and paleo-channel data, a mixing model was used to generate  
 305 Gaussian mixture distributions that were fitted to both the 164,520 detrended terrace elevation points and the median discharges  
 306 estimated for the 79 paleo-channel segments (Fig. 109). Results are used to determine if Deweyville terraces should be divided  
 307 into three distinct sets. The Akaike Information Criterion (AIC) and Bayesian Information Criterion (BIC) were applied to  
 308 both mixing models in order to optimize the number of components used to represent each distribution (Fig. 109C & 109D).  
 309 Two and three components were selected for the distributions of detrended elevation points and median paleo-channel  
 310 discharges, respectively (Fig. 9A, 10A & 109B).



311  
 312 **Figure 109.** Mixing model fits to measured distributions of terrace elevation and estimated paleo-discharges. Distributions using (A)  
 313 elevation and (B) paleo-channels support an interpretation of allogenic forcing for high terrace abandonment due to increasing  
 314 discharge. Akaike Information Criterion (AIC) for (C) detrended elevation and (D) paleo-discharge mixing model. BIC results are  
 315 not shown here but have similar trends to AIC. AIC results are shown for the mixing model that are solved for a diagonal and full

316 covariance matrix and shared and unshared covariance. The model also used a small Regularization value to ensure the estimated  
317 covariance matrix is positive.

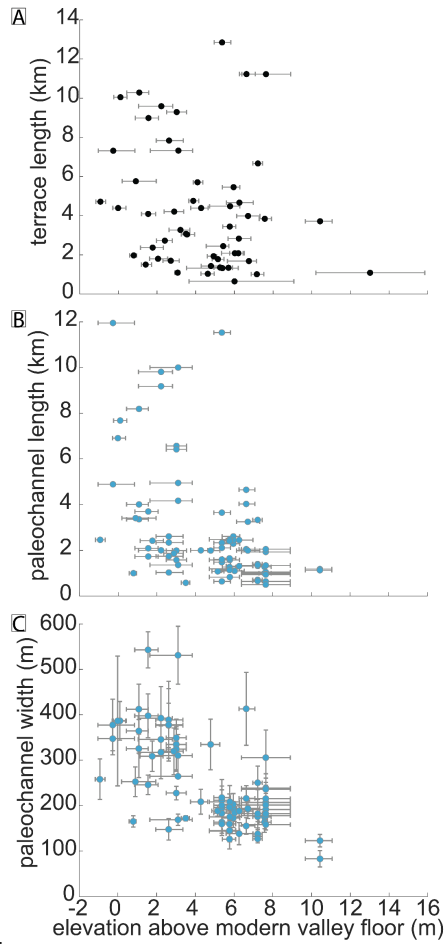
318 An important additional measurement used to assess whether terraces were abandoned due to enhanced local incision  
319 driven by gradient change during channel bend cut-off was the elevation differences between 40 adjacent terraces. These  
320 connections can first be assessed by comparing the minimum bounding box length of terraces, paleo-channel width, and paleo-  
321 channel length (Fig. 4011). These measured elevation differences between terraces were compared to estimated elevation  
322 changes produced by bend cut-offs. We used Eq. 2 to calculate the elevation drop produced by a bend cutoff as:

$$\Delta elevation_{bend\ cutoff} = length_{bend} * slope_{channel} \quad (2)$$

323 On several low, intermediate, and high Deweyville terraces, the lengths of paleo-channels that had one bend preserved were  
324 measured using the bare-earth DEM (e.g., Fig. 2). The mean and standard deviations for bend lengths on the low, intermediate  
325 and high terraces are  $5.7 \pm 2.8$  km (n = 3),  $4.6 \pm 3.0$  km (n = 10), and  $2.3 \pm 1.1$  km (n = 11), respectively. The overall distribution  
326 above the modern valley floor of paleochannel lengths plotted in Figure 10B11B. We approximated channel slope using the  
327 planes fit to the terrace elevation points for each classification. The calculated mean slope and standard error for the low,  
328 intermediate, and high terraces are  $3.0 \times 10^{-4}$  ( $3.1 \times 10^{-6}$ ),  $2.9 \times 10^{-4}$  ( $1.1 \times 10^{-6}$ ), and  $3.0 \times 10^{-4}$  ( $1.2 \times 10^{-6}$ ), respectively. Using

Formatted: Font: Bold

329 Equation 2, estimated elevation drops driven by a possible bend cut-off are  $1.6 \pm 0.8$  m,  $1.3 \pm 0.9$  m, and  $0.7 \pm 0.3$  m (Fig.

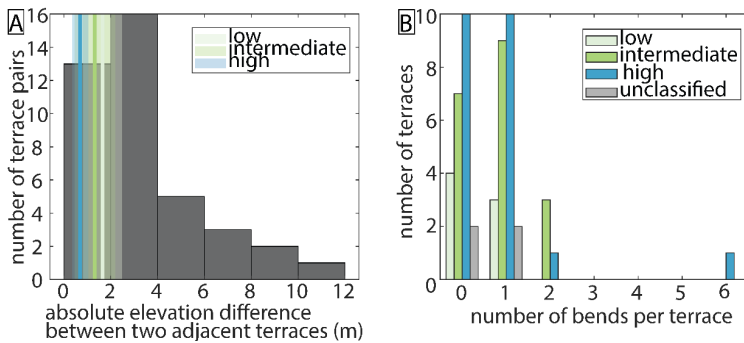


330 [4911A](#).

331 Figure 4911 (A) terrace length, (B) paleo-channel length, and (C) paleo-channel width plotted along the median elevation of the  
332 associated terrace above the modern valley floor plane. The youngest terraces are more likely to have larger terrace lengths as well

333 as paleochannel lengths. Terrace length was measured as the longest length of a minimum bounding box envelop for each terrace.  
 334 These envelopes were defined with edges in the N-S and E-W direction. Error bars show the interquartile range of each terrace.

335 An additional measurement used to evaluate the likelihood of terraces being produced by bend cut-off was the largest  
 336 number of channel bends present in a segment of paleo-channel preserved on a terrace surface. The number of channel bends  
 337 preserved on terrace surfaces can be used as an indicator for autogenic versus allogenic processes, whereby allogenic terrace  
 338 formation likely abandons larger paleo-floodplain sections, preserving multiple channel bends. For incising rivers, the  
 339 autogenic cut off of a single meander bend has been shown to be sufficient to produce the enhanced channel erosion required  
 340 to elevate relatively small sections of the previous active floodplain above flood levels (Finnegan and Dietrich, 2011).



341  
 342 **Figure 14.12.** Terrace properties used to assess the likelihood of meander bend-cutoff being the driver of terrace formation. (A)  
 343 Differences in elevation between adjacent terrace surfaces. Also plotted as vertical lines and swaths are the mean values  $\pm 1$  standard  
 344 deviation for elevation decreases expected from cutting off a single meander bend for paleo-channels of the low, intermediate, and  
 345 high Deweyville ~~At~~ ~~group~~ ~~bounding~~ ~~surfaces~~. (B) Maximum number of paleo-meander bends preserved in a channel segment on  
 346 each terrace. Most terraces have between 0-1 channel bends preserved for one generation of channel. Only intermediate and high  
 347 Deweyville terraces have more than two channel bends preserved by a paleo-channel.

#### 348 4. Summary of observations

349 We mapped 52 terraces and 79 paleo-channel segments in the study area (Fig. 1B). Of these terraces, 22 are classified  
 350 as high Deweyville, 19 as intermediate Deweyville, 8 as low Deweyville, and 4 were left unclassified as they could not be  
 351 correlated with terraces mapped by either Blum et al. (1995) or Garvin (2008). The low, intermediate, and high Deweyville  
 352 terraces have median values for detrended elevations of 0.03 m, 2.06 m, and 6.37 m. Based on our mixture modeling, the mean  
 353 and standard deviation of the detrended elevation components are  $5.6 \pm 4.18$  m and  $1.32 \pm 2.19$  m with mixing proportions of  
 354 0.51 and 0.49, respectively. Similarly, the mean and standard deviation for the three Gaussian distributions describing paleo-  
 355 discharges are  $795 \pm 80$  m<sup>3</sup>/s,  $2083 \pm 139$  m<sup>3</sup>/s, and  $4013 \pm 21$  m<sup>3</sup>/s with mixing proportions of 0.68, 0.30, and 0.02,  
 356 respectively. Terraces vary in both size and shape, although they are typically elongate parallel to the valley axis and continuous  
 357 for less than 10 km in that direction. The distribution of terraces is asymmetric, with more terraces observed on the east side

358 of the valley (**Fig. 1B**). Consequently, most terraces are unpaired, meaning they have no topographic equivalent on the opposite  
359 side of the valley.

360 The best-fit planes to elevations for the Deweyville terrace groups defined by Blum et al. (1995), Garvin (2008), and  
361 Hidy et al. (2014) show remarkably similar slopes amongst terrace sets. The slopes and standard error for the low, intermediate,  
362 and high terraces are  $3.0 \times 10^{-4}$  ( $3.1 \times 10^{-6}$ ),  $2.9 \times 10^{-4}$  ( $1.10 \times 10^{-6}$ ), and  $3.0 \times 10^{-4}$  ( $1.2 \times 10^{-6}$ ), respectively. These paleo-slopes are  
363 indistinguishable from the estimated slope for the modern valley of  $3.0 \times 10^{-4}$  ( $8.0 \times 10^{-8}$ ) (**Fig. 3A4A**). It is not surprising that  
364 all four profiles are well fit by planes given the fact that the studied river segment represents less than ten percent of the modern  
365 river length and both grain size and discharge vary little over the studied reach.

366 Plane fits for the low, intermediate, and high Deweyville terrace sets have RMSEs of 1.43m, 1.54m, and 1.41m,  
367 respectively. Values of RMSE for best-fit planes to randomly grouped terraces are sensitive to the number of terraces defining  
368 a group. The fewer the number of terraces, the more likely it is that a low RMSE will result (**Fig. 76**). It is therefore important  
369 when comparing randomly grouped terraces to the previously classified groups that the number of terraces in each be the same.  
370 Running our analysis of 50,000 sets of randomly assembled terraces with the same number of elements as the low ( $n=8$ ),  
371 intermediate ( $n=19$ ) and high ( $n=22$ ) Deweyville groups yielded the following RMSE results. The median and interquartile  
372 values of RMSE for planes fit to randomly selected terraces of the number present in the low-terrace classification are 1.82m,  
373 1.55m, and 2.21m. The median and interquartile values of RMSE for planes fit to randomly selected terraces of the number  
374 present in the intermediate-terrace classification are 2.41m, 2.15m, and 2.66m. And finally, the median and interquartile values  
375 of RMSE for planes fit to randomly selected terraces of the number present in the high-terrace classification are 2.49m, 2.25m,  
376 and 2.71m.

377 The RMSE values for the best-fit planes to the classified Deweyville terraces are plotted on their associated synthetic  
378 RMSE distributions for randomly selected terraces in **Fig. 67**. Inspection of **Fig. 76** reveals little overlap between the classified  
379 high terraces and the random samplings of terraces. For the high Deweyville case, there was only a 0.008% occurrence of  
380 randomly selected terraces yielding an RMSE as low as 1.41m. A very different result was found for the classified low terraces,  
381 where its RMSE falls well within the associated distribution of synthetic RMSEs with fully 21% of all randomly selected cases  
382 having lower RMSE values. Minimal overlap was found between the RMSE for the classified intermediate terraces and the  
383 distribution of RMSE values generated from random terrace groupings. Only 1% of the randomly selected sets terraces were  
384 better fit to a plane than the classified group of intermediate terraces. Mapped paleo-channels have widths that range from 82  
385 to 543 m (**Fig. 87**). Estimated bankfull discharges calculated using these widths (**Eq. 1**) range from 233  $\text{m}^3/\text{s}$  to more than  
386 4000  $\text{m}^3/\text{s}$  (**Fig. 98**). These paleo-discharges cluster into two groups, one at lower discharges centered around  $795 \pm 80 \text{ m}^3/\text{s}$   
387 and one at higher discharges centered on  $2083 \pm 139 \text{ m}^3/\text{s}$  (**Fig. 109B**). The grouping of lower-discharge paleo-channels sit on  
388 terraces that have median elevations  $>4.5$  m above the modern valley floor and correspond to high Deweyville terraces (**Fig.**  
389 **98**). The grouping of higher-discharge paleo-channels is preserved on terraces that have median elevations from 0.2 m below  
390 to 5.2 m above the modern floodplain and correspond to both intermediate and low Deweyville terraces (**Fig. 98**). The  
391 investigation of paleo-channel characteristics revealed that paleo-channel widths, paleo-channel lengths, and overall terrace

392 lengths all are more likely to be greater for younger terraces (Fig. 4011). Most terraces have one or fewer channel bends  
393 preserved (Fig. 124B) and only the intermediate and high Deweyville classifications possess terraces with more than two  
394 preserved channel bends.

## 395 5 Discussion and Conclusions

396 Late Pleistocene terraces of the lower Trinity River valley formed during a period of net sea-level fall punctuated by  
397 shorter and smaller magnitude fluctuations (Anderson et al., 2016). Previous researchers have interpreted the formation of the  
398 Trinity terraces, as well as those observed in other Texas coastal valleys, in the context of these fluctuations (Blum et al., 1995;  
399 Blum and Aslan, 2006; Morton et al., 1996; Rodriguez et al., 2005). However, it has also been suggested that this terrace  
400 formation in the lower Trinity River valley was driven by autogenic triggers (Guerit et al., 2020). The motivation for this study  
401 was to develop tools to help distinguish between these two forcings that can produce terraces.

402 Several morphological characteristics exist to describe both the Trinity River terraces and their associated paleo-  
403 channels. The terraces are most commonly unpaired (Fig. 1), which is expected during autogenic terrace formation associated  
404 with unsteady lateral migration rates during formation (Bull, 1990; Merritts et al., 1994) and river bend cut-off (Finnegan and  
405 Dietrich, 2011). On the flip side, paired terraces can also be formed during constant, albeit low vertical incision rates, during  
406 lateral migration (Limaye and Lamb, 2016). Unpaired terraces can also be produced by unequal lateral river erosion post  
407 terrace formation that preferentially removes half of a previously formed pair of allogenic terraces (Malatesta et al., 2017).  
408 Similarly, lateral migration also affects the age distribution of the terraces preserved because younger terraces, closer to the  
409 modern river are more likely to eroded away than older terraces (Lewin and Macklin, 2003; Limaye and Lamb, 2016). The  
410 presence of unpaired terraces in the lower Trinity River valley may therefore be most indicative of the relative importance of  
411 lateral migration for this system.

412 For the Trinity River, many of the valley-ward edges of the lower and intermediate Deweyville Allogroups-bounding  
413 surfaces have the shapes of meander bends, recording the most outward extent of the active channel before the floodplain  
414 surface was abandoned (Fig. 1, Fig. 2). We take this as evidence for the autogenic process of channel cutoff triggering terrace  
415 formation. The observed elevation differences between adjacent terraces are also consistent with those predicted by cut off of  
416 a single meander bend (Fig. 4A12A). Similar interpretations have also been made for strath terraces in bedrock (Finnegan  
417 and Dietrich, 2011). Furthermore, their tendency to be preserved as unpaired terraces with a small number (< 2) of channel  
418 bends is more consistent with the stochastic nature of meander cutoffs by autogenic processes than large-scale incisional events  
419 due to allogenic forcings (Fig. 4A-12A & 4B12B, Finnegan and Dietrich, 2011). Therefore, the morphology of the Trinity  
420 River valley terraces alone is suggestive of an autogenic forcing, but likely not sufficient to distinguish between allogenic  
421 versus autogenic terrace formation.

422 We argue that a robust test for assessing the likelihood of autogenic versus allogenic forcing in terrace formation  
423 comes from an analysis of the topographic variability of terrace sets inferred to have formed synchronously. Here we have  
424 developed a method to quantitatively compare elevation variability of any classified group of terraces against randomly

425 selected terrace sets (Fig. 56, Fig. 67) so that we can evaluate whether a classified group is better organized than arbitrarily  
426 selected ones. For the lower Trinity River valley, if the Deweyville terraces formed synchronously (Blum et al., 1995; Blum  
427 and Aslan, 2006; Morton et al., 1996; Rodriguez et al., 2005), one would predict that terraces within these groups would show  
428 lower variation about a best-fit plane than randomly grouped terraces (Fig. 67). Limaye and Lamb (2016) defined a unique  
429 elevation set as surfaces that are separated by more than 1m. They found that lateral migration during a constant incision rate  
430 versus pulsed incision rates can result in similar and indistinguishable terrace sets (Limaye and Lamb, 2016). Our approach  
431 builds on this idea and develops a framework that evaluates the magnitudes of variations in elevation amongst terraces  
432 compared to a fitted plane for the set. This approach is especially useful for studies where age control across terraces is not  
433 well constrained. Since we are assessing many elevation points from each terrace in the terrace set, it is possible to tease apart  
434 long profile variations for terrace sets only vertically separated by ~1m.

435 Our RMSE results show that the best-fit plane for the low Deweyville [Allogroup-bounding surface](#) cannot be separated  
436 from, and is instead consistent with, sets of randomly grouped terraces mimicking autogenic processes of either bend cutoff or  
437 of unsteady river lateral migration during constant base level fall (Fig. 6B7B). The driver for the intermediate Deweyville  
438 [Allogroup-bounding surface](#) cannot be unambiguously determined based on the RMSE analysis. The classified group is better  
439 organized than most, but not all, randomly generated groupings of terraces (Fig. 6C7C). The overlap leads us to presume that  
440 the null hypothesis of autogenic terrace formation cannot be robustly falsified. A different conclusion was reached for the high  
441 Deweyville [bounding surface](#)[Allogroup](#). With our RMSE analysis, we reject the null hypothesis of autogenic terrace formation.  
442 The high Deweyville [Allogroup-bounding surface](#) is most likely the product of punctuated allogenic change with an RMSE  
443 that is as small as any of the 50,000 values generated for random groupings of terraces (Fig. 6A7A). A difference between the  
444 low/intermediate versus high terraces was also found in the distribution of detrended terrace elevations using a 2 component  
445 Gaussian mixing model. The first component of this model overlaps with elevations classified as low and intermediate  
446 Deweyville, while the second component corresponds most closely to high Deweyville elevations (Fig. 45, Fig. 109A). We,  
447 therefore, conclude that the high Deweyville terraces are different than the other two sets and record an allogenic signal  
448 connected with early valley incision. This new analysis likely means that across a relatively short interval of time, <10 kyr,  
449 terraces on the Trinity River switched from recording an allogenic trigger in the high Deweyville [Allogroup-bounding surface](#)  
450 to being indistinguishable from terraces formed by autogenic triggers such as bend cut-off or unsteady lateral migration rates.

451 The connections between potential discharge changes and terrace formation were assessed using paleo-channel widths  
452 and grain size (Fig. 98, Fig. 109B). Paleo-channel discharge estimates reveal a factor of two increase in bankfull discharge  
453 moving from older, high Deweyville terraces to younger, intermediate, and low Deweyville terraces. The estimated changes  
454 through time in bankfull discharge are not matched by estimated changes in river long-profile or paleo-slope. Previously  
455 discussed best-fit planes to the Deweyville [Allogroups-bounding surface](#) have slopes that are roughly constant and  
456 indistinguishable from the modern long profile for the Trinity River (Fig. 3A4A). Theory by Parker et al. (1998) and  
457 experiments by Whipple et al., (1998) have demonstrated long-profile slope for sandy fluvial systems is a function of sediment-  
458 to-water discharges. Terraces associated with base-level fall have been shown to maintain consistent valley slopes (Tofelde et

459 al., 2019). Experiments by the same authors also showed that sediment and/or water discharge changes produce changing  
460 slopes for terrace sets, which we do not observe here. We suspect that the switch in discharge is not directly recorded in the  
461 terrace elevation because the change in water discharge appears to have been approximately matched by a sediment-flux  
462 increase, as recorded in the constant long-profile slope for the paleo-river. With no slope reduction, no incision would have  
463 occurred. As a result, discharge changes recorded by segments of paleo-channels on the intermediate and low Deweyville  
464 terraces are not interpreted to have driven incision and terrace formation. Instead, it likely that an autogenic trigger associated  
465 with persistent base-level fall drove the terracing. Recent synthesis studies by Phillips and Jerolmack (2016) and Dunne and  
466 Jerolmack (2018) confirm that these estimates of bankfull discharge are tied to moderate flooding and representative of mean  
467 climate properties. While our estimated discharge changes over the latest Pleistocene are large, it is only half of the proposed  
468 four times increase reported for similar paleo-channels preserved on terraces of the nearby lower Brazos River valley (Sylvia  
469 and Galloway, 2006).

470 Maintenance of a roughly constant slope while water discharge changed therefore almost certainly required  
471 commensurate changes to sediment discharge. We can test this change in sediment discharge by looking at results from existing  
472 studies. An increase in sediment discharge is in agreement with Anderson (2005), who suggests that sediment discharge was  
473 greater during the LGM than today. However, calculations for the Trinity River by other authors do not currently reflect these  
474 changes. Sediment discharges have been estimated to decrease during the LGM (intermediate and low Deweyville) based on  
475 the BAQRT model by Syvitski and Milliman (2007) (Blum and Hattier-Womack, 2009; Garvin, 2008). Hidy et al. (2014) also  
476 calculated  $^{10}\text{Be}$  denudation rates and suggested that upstream weathering was greater during the interglacial periods and that  
477 reworking of stored sediments was greater during glacial periods. However, Hidy et al. (2014) was not able to combine the  
478 effects of reworking and upstream sediment flux using  $^{10}\text{Be}$  to estimate the sediment discharge associated with terrace  
479 formation. More recent methods were developed to estimate sediment discharge based on bedforms and stratigraphy, which  
480 are exposed along the Trinity River (Mahon and McElroy, 2018). Therefore, there is also an opportunity to refine and improve  
481 sediment discharge estimates for Deweyville terraces. Regardless, responsive adjustments to sediment discharge suggest that  
482 throughout the latest Pleistocene, the river itself remained a predominantly transport limited system (Howard, 1980; Whipple,  
483 2002).

484 Understanding the cut off of a river bend is important to identify autogenic triggers for terrace formation. We have  
485 shown that a majority of Deweyville terraces in the Trinity valley preserve no more than a single paleo-channel bend (**Fig.**  
486 **H-B12B**) and that elevation differences between adjacent terraces are similar to an expected elevation change driven by channel  
487 shortening through cut off to a river bend (**Fig. H-A12A**). These terrace properties highlight an opportunity for our community  
488 to measure the number of bends involved in the autogenic shortening of river channels. Specifically, there is an opportunity to  
489 quantify what percentage of cutoffs result in two or more bends being detached from the active channel in short amounts of  
490 time, thereby refining an expected upper limit to the number of channel bends preserved on autogenically generated terraces.  
491 Exceptionally preserved paleo-channels such as on the Trinity River, provide this opportunity to distinguish autogenic  
492 processes responsible for terrace formation, and as such might provide a more faithful record of changes in discharge to the

493 system than terrace elevations and morphologies. An additional mechanism for reducing uncertainty in the processes that cut  
494 Trinity terraces would be assembling a greater number of terrace ages. Increasing age control could constrain vertical versus  
495 lateral migration rates for the river to a point where autogenic versus allogenic processes connected to terrace formation are  
496 separable (Limaye and Lamb, 2016; Merritts et al., 1994).

497 Irrespective of terraces formation, other river systems across the southeastern United States have the potential to also  
498 record a step-increase in formative discharge seen in the Trinity valley between the high to intermediate/low Deweyville  
499 terraces. This change was likely driven by a wetter climate in southeast Texas during the period ~34–20 ka, based on OSL  
500 dates for the low and intermediate Deweyville terraces (Garvin, 2008). During the Last Glacial Maximum (19-26 ka),  
501 precipitation in western and southwestern USA has been shown to be ~0.75–1.5 and ~1.3-1.6 of modern, respectively (Ibarra  
502 et al., 2018). Additionally, GCM models show a general increase in precipitation in the study area during the late Pleistocene  
503 (Roberts et al., 2014 (Fig. 2); McGee et al., 2018 (Fig. 2)). Our observations agree with other workers who interpreted the  
504 changes in channel size as an increase in mean discharge during this period (Alford and Holmes, 1985; Gagliano and Thom,  
505 1967; Saucier and Fleetwood, 1970; Sylvia and Galloway, 2006). Observations of larger paleo-channels during this period are  
506 also seen across rivers in the southeast of Texas (e.g. Bernard, 1950; Blum et al., 1995; Sylvia and Galloway, 2006), Arkansas  
507 and Louisiana (e.g. Saucier and Fleetwood, 1970), and Georgia and South Carolina (e.g. Leigh and Feeney, 1995; Leigh et al.,  
508 2004; Leigh, 2008).

509 Our contribution to the existing work on terraces in this region is to reconcile the literature that suggests an episodic  
510 cut and fill and/or base level change model (Blum et al., 1995) with the literature on terrace formation due to increased  
511 discharge (Sylvia and Galloway, 2006). While both have the potential to generate terraces, intrinsic processes such as bend  
512 cut-off and unsteady lateral migration during constant base level fall need to first be ruled out. For example, relatively slow  
513 vertical incision rates especially, pulsed discharge changes (allogenic process) and unsteady lateral migration (autogenic  
514 process) showed indistinguishable morphologies in Limaye and Lamb (2016). Here, for all but the high Deweyville, autogenic  
515 triggers for terrace development cannot be ruled out.

516 The results presented here demonstrate that it is critical to understand the many potential forcings (both allogenic and  
517 autogenic) on a river system that can lead to terrace formation and to employ robust, quantitative tests for discriminating  
518 between these forcings before using terraces to reconstruct paleo-environmental histories. The method proposed here for  
519 assessing the role of allogenic processes in terrace formation using the variability of terrace elevations provides a simple,  
520 quantitative test, and may prove useful for interpreting terrace formation in other river systems. We were not able to correlate  
521 terrace levels back to distinct trigger events, although allogenic forcings such as sea-level fluctuations and discharge changes  
522 were also classified here. We suggest that paleo-channel characteristics are a more faithful record of discharge changes in  
523 fluvial systems and that additional bend metrics ~~introduce~~ can differentiate autogenic terrace formation processes, specifically  
524 bend cut-off from unsteady lateral migration rates.

525 **Data availability**

526 The lidar dataset was acquired from the Texas Natural Resource Information System (TNRIS) at <https://tnris.org>. Please see  
527 the reference to each dataset. Tables with analysis produced from the lidar datasets are included in the supplementary material.

528 **Author contribution**

529 All authors designed the analysis and contributed to the manuscript writing. HHG and TE analyzed the lidar dataset. TG  
530 developed the code to fit planes to the lidar dataset.

531 **Competing interests**

532 The authors declare that they have no conflict of interest.

533 **Acknowledgments**

534 We thank Webster Mangham for providing the report from the Trinity River Authority of Texas Phase II, Bathymetry and  
535 Sediment Collection for the Port of Liberty Study. We thank Ajay Limaye and one anonymous reviewer and Ajay Limaye for  
536 constructive reviews. We also thank Joel Johnson and Gary Kocurek for insightful comments on early versions of the  
537 manuscript as well as Niels Hovius, Mike Lamb, Paola Passalacqua, and Daniella Rempe for additional comments. HHG was  
538 funded by the Jackson School of Geoscience Recruiting Fellowship and the National Science Foundation Graduate Research  
539 Fellowship.

540 **References**

- 541 Alford, J. J. and Holmes, J. C.: Meander Scars as Evidence of Major Climate Change in Southwest Louisiana, *Ann. Assoc.*  
542 *Am. Geogr.*, 75(3), 395–403, doi:10.1111/j.1467-8306.1985.tb00074.x, 1985.
- 543 Anderson, J. B., Wallace, D. J., Simms, A. R., Rodriguez, A. B. and Milliken, K. T.: Variable response of coastal environments  
544 of the northwestern Gulf of Mexico to sea-level rise and climate change: Implications for future change, *Mar. Geol.*, 352, 348–  
545 366, doi:10.1016/j.margeo.2013.12.008, 2014.
- 546 Anderson, J. B., Wallace, D. J., Simms, A. R., Rodriguez, A. B., Weight, R. W. R. and Taha, Z. P.: Recycling sediments  
547 between source and sink during a eustatic cycle: Systems of late Quaternary northwestern Gulf of Mexico Basin, *Earth-Science*  
548 *Rev.*, 153, 111–138, doi:10.1016/j.earscirev.2015.10.014, 2016.
- 549 Baker, E. T. J.: Stratigraphic Nomenclature and Geologic Sections of the Gulf, U.S. Geol. Surv. Open-File Rep., 94–461, 34,  
550 1995.

551 Bernard, H. A.: Quaternary Geology of Southeast Texas, LSU Historical Dissertations and Theses 7952., 1950.

552 Blom, A., Arksteijn, L., Chavarrías, V. and Viparelli, E.: The equilibrium alluvial river under variable flow and its channel-  
553 forming discharge, *J. Geophys. Res. Earth Surf.*, 122(10), 1924–1948, doi:10.1002/2017JF004213, 2017.

554 Blum, M., Martin, J., Milliken, K. and Garvin, M.: Paleovalley systems: Insights from Quaternary analogs and experiments,  
555 *Earth-Science Rev.*, 116(1), 128–169, doi:10.1016/j.earscirev.2012.09.003, 2013.

556 Blum, M. D. and Aslan, A.: Signatures of climate vs. sea-level change within incised valley-fill successions: Quaternary  
557 examples from the Texas GULF Coast, *Sediment. Geol.*, 190(1–4), 177–211, doi:10.1016/j.sedgeo.2006.05.024, 2006.

558 Blum, M. D. and Törnqvist, T. E.: Fluvial responses to climate and sea-level change: A review and look forward,  
559 *Sedimentology*, 47(SUPPL. 1), 2–48, doi:10.1046/j.1365-3091.2000.00008.x, 2000.

560 Blum, M. D., Morton, R. A. and Durbin, J. M.: “Deweyville” Terraces and Deposits of the Texas Gulf Coastal Plain, *GCAGS*  
561 *Trans.*, 45(1950), 53–60, 1995.

562 Bull, W. B.: Stream-terrace genesis: implications for soil development, *Geomorphology*, 3(3–4), 351–367, doi:10.1016/0169-  
563 555X(90)90011-E, 1990.

564 Church, M.: Bed Material Transport and the Morphology of Alluvial River Channels, *Annu. Rev. Earth Planet. Sci.*, 34(1),  
565 325–354, doi:10.1146/annurev.earth.33.092203.122721, 2006.

566 Daley, J. and Cohen, T.: Climatically-Controlled River Terraces in Eastern Australia, *Quaternary*, 1(3), 23,  
567 doi:10.3390/quat1030023, 2018.

568 Erkens, G., Dambeck, R., Volleberg, K. P., Bouman, M. T. I. J., Bos, J. A. A., Cohen, K. M., Wallinga, J. and Hoek, W. Z.:  
569 Fluvial terrace formation in the northern Upper Rhine Graben during the last 20 000 years as a result of allogenic controls and  
570 autogenic evolution, *Geomorphology*, 103(3), 476–495, doi:10.1016/j.geomorph.2008.07.021, 2009.

571 FEMA: FEMA 2011 1m Liberty Lidar, 2011.

572 Finnegan, N. J. and Dietrich, W. E.: Episodic bedrock strath terrace formation due to meander migration and cutoff, *Geology*,  
573 39(2), 143–146, doi:10.1130/G31716.1, 2011.

574 Gagliano, S. M. and Thom, B. G.: Deweyville Terrace, Gulf and Atlantic Coasts. Technical Report 39., Baton Rouge., 1967.

575 Galloway, W. E., Ganey-Curry, P. E., Li, X. and Buffler, R. T.: Cenozoic depositional history of the Gulf of Mexico basin,  
576 *Am. Assoc. Pet. Geol. Bull.*, 84(11), 1743–1774, doi:10.1306/8626C37F-173B-11D7-8645000102C1865D, 2000.

577 Garvin, M. G.: Late Quaternary geochronologic, stratigraphic, and sedimentologic framework of the Trinity River incised  
578 valley: East Texas coast, , (December), 2008.

579 Guerit, L., Foreman, B. Z., Chen, C., Paola, C. and Castelltort, S.: Autogenic delta progradation during sea-level rise within  
580 incised valleys, *Geology*, XX(Xx), 1–5, doi:10.1130/g47976.1, 2020.

581 Hancock, G. S. and Anderson, R. S.: Numerical modelling of fluvial strath terrace formation in response to oscillating climate,  
582 *Geol. Soc. Am. Bull.*, 114(9), 1131–1142, doi:10.1130/0016-7606(2002)114<1131, 2002.

583 Heinrich, P., Miner, M., Paulsell, R. and McCulloh, R.: Response of Late Quaternary Valley systems to Holocene sea level  
584 rise on continental shelf offshore Louisiana: preservation potential of paleolandscapes, , (February), 104, 2020.

585 Hidy, A. J., Gosse, J. C., Blum, M. D. and Gibling, M. R.: Glacial-interglacial variation in denudation rates from interior  
586 Texas, USA, established with cosmogenic nuclides, *Earth Planet. Sci. Lett.*, 390, 209–221, doi:10.1016/j.epsl.2014.01.011,  
587 2014.

588 Howard, A. D.: Thresholds in river regimes, in *Thresholds in geomorphology*, pp. 227–258., 1980.

589 Ibarra, D. E., Oster, J. L., Winnick, M. J., Rugenstein, J. K. C., Byrne, M. P. and Chamberlain, C. P.: Warm and cold wet states  
590 in the western United States during the Pliocene-Pleistocene, *Geology*, 46(4), 355–358, doi:10.1130/G39962.1, 2018.

591 Knox, J. C.: Responses of floods to Holocene climatic change in the upper Mississippi Valley, *Quat. Res.*, 23(3), 287–300,  
592 doi:10.1016/0033-5894(85)90036-5, 1985.

593 Lane, E. W.: Design of Stable Channels, *Trans. Am. Soc. Civ. Eng.*, 120(1), 1234–1260, doi:10.1061/TACEAT.0007188,  
594 1955.

595 Leigh, D. S.: Late Quaternary climates and river channels of the Atlantic Coastal Plain, Southeastern USA, *Geomorphology*,  
596 101(1–2), 90–108, doi:10.1016/j.geomorph.2008.05.024, 2008.

597 Leigh, D. S. and Feeney, T. P.: Paleochannels indicating wet climate and lack of response to lower sea level, southeast Georgia,  
598 *Geology*, 23(8), 687–690, doi:10.1130/0091-7613(1995)023<0687:PIWCAL>2.3.CO;2, 1995.

599 Leigh, D. S., Srivastava, P. and Brook, G. A.: Late Pleistocene braided rivers of the Atlantic Coastal Plain, USA, *Quat. Sci.*  
600 *Rev.*, 23(1–2), 65–84, doi:10.1016/S0277-3791(03)00221-X, 2004.

601 Lewin, J. and Macklin, M. G.: Preservation potential for late quaternary river alluvium, *J. Quat. Sci.*, 18(2), 107–120,  
602 doi:10.1002/jqs.738, 2003.

603 Limaye, A. B. S. and Lamb, M. P.: Numerical simulations of bedrock valley evolution by meandering rivers with variable  
604 bank material, *J. Geophys. Res. Earth Surf.*, 119(4), 927–950, doi:10.1002/2013JF002997, 2014.

605 Limaye, A. B. S. and Lamb, M. P.: Numerical model predictions of autogenic fluvial terraces and comparison to climate  
606 change expectations, *J. Geophys. Res. Earth Surf.*, 121(3), 512–544, doi:10.1002/2014JF003392, 2016.

607 Mackey, B. H., Roering, J. J. and Lamb, M. P.: Landslide-dammed paleolake perturbs marine sedimentation and drives genetic  
608 change in anadromous fish, *Proc. Natl. Acad. Sci. U. S. A.*, 108(47), 18905–18909, doi:10.1073/pnas.1110445108, 2011.

609 Malatesta, L. C., Prancevic, J. P. and Avouac, J. P.: Autogenic entrenchment patterns and terraces due to coupling with lateral  
610 erosion in incising alluvial channels, *J. Geophys. Res. Earth Surf.*, 122(1), 335–355, doi:10.1002/2015JF003797, 2017.

611 McGee, D., Moreno-Chamorro, E., Marshall, J. and Galbraith, E. D.: Western U.S. lake expansions during Heinrich stadials  
612 linked to Pacific Hadley circulation, *Sci. Adv.*, 4(11), 1–11, doi:10.1126/sciadv.aav0118, 2018.

613 Merritts, D. J., Vincent, K. R. and Wohl, E. E.: Long river profiles, tectonism, and eustasy: A guide to interpreting fluvial  
614 terraces, *J. Geophys. Res. Solid Earth*, 99(B7), 14031–14050, doi:10.1029/94JB00857, 1994.

615 Molnar, P., Brown, E. T., Burchfiel, B. C., Deng, Q., Feng, X., Li, J., Raisbeck, G. M., Shi, J., Zhangming, W., Yiou, F. and  
616 You, H.: Quaternary Climate Change and the Formation of River Terraces across Growing Anticlines on the North Flank of  
617 the Tien Shan, China, *J. Geol.*, 102(5), 583–602, doi:10.1086/629700, 1994.

618 Morton, R. A., Blum, M. D. and White, W. A.: Valley Fills of Incised Coastal Plain Rivers, Southeastern Texas, Gulf Coast

619 Assoc. Geol. Soc., 46, 321–331, doi:10.1306/2DC40B2D-0E47-11D7-8643000102C1865D, 1996.

620 Muto, T. and Steel, R. J.: Autogenic response of fluvial deltas to steady sea-level fall: Implications from flume-tank  
621 experiments, *Geology*, 32(5), 401–404, doi:10.1130/G20269.1, 2004.

622 Parker, G., Paola, C., Whipple, K. X. and Mohrig, D.: Alluvial Fans Formed by Channelized Fluvial and Sheet Flow. I: Theory,  
623 *J. Hydraul. Eng.*, 124(10), 985–995, doi:10.1061/(ASCE)0733-9429(1998)124:10(985), 1998a.

624 Parker, G., Paola, C., Whipple, K. X. and Mohrig, D.: Alluvial Fans Formed by Channelized Fluvial and Sheet Flow. I: Theory,  
625 *J. Hydraul. Eng.*, 124(10), 985–995, doi:10.1061/(ASCE)0733-9429(1998)124:10(985), 1998b.

626 Pazzaglia, F. J.: Fluvial Terraces, in *Treatise on Geomorphology*, vol. 9, pp. 379–412., 2013.

627 Pazzaglia, F. J. and Gardner, T. W.: Fluvial terraces of the lower Susquehanna River, *Geomorphology*, 8(2–3), 83–113,  
628 doi:10.1016/0169-555X(93)90031-V, 1993.

629 Pazzaglia, F. J., Gardner, T. W. and Merritts, D. J.: Bedrock fluvial incision and longitudinal profile development over geologic  
630 time scales determined by fluvial terraces, pp. 207–235., 1998.

631 Roberts, W. H. G., Valdes, P. J. and Payne, A. J.: Topography's crucial role in Heinrich Events, *Proc. Natl. Acad. Sci. U. S.*  
632 *A.*, 111(47), 16688–16693, doi:10.1073/pnas.1414882111, 2014.

633 Rodriguez, A. B., Anderson, J. B. and Simms, A. R.: Terrace Inundation as an Autocyclic Mechanism for Parasequence  
634 Formation: Galveston Estuary, Texas, U.S.A., *J. Sediment. Res.*, 75(4), 608–620, doi:10.2110/jsr.2005.050, 2005.

635 Saucier, R. T.: *Geomorphology and Quaternary Geologic History of the Lower Mississippi Valley*, US Army Corps Eng., I,  
636 1–414, 1994.

637 Saucier, R. T. and Fleetwood, A. R.: Origin and Chronologic Significance of Late Quaternary Terraces, Ouachita River,  
638 Arkansas and Louisiana, *GSA Bull.*, 81(3), 869–890, doi:10.1130/0016-7606(1970)81[869:OACSOL]2.0.CO;2, 1970.

639 Simms, A. R., Anderson, J. B., Milliken, K. T., Taha, Z. P. and Wellner, J. S.: Geomorphology and age of the oxygen isotope  
640 stage 2 (last lowstand) sequence boundary on the northwestern Gulf of Mexico continental shelf, *Geol. Soc. Spec. Publ.*, 277,  
641 29–46, doi:10.1144/GSL.SP.2007.277.01.03, 2007.

642 Smith, V. B. and Mohrig, D.: Geomorphic signature of a dammed Sandy River: The lower Trinity River downstream of  
643 Livingston Dam in Texas, USA, *Geomorphology*, 297, 122–136, doi:10.1016/j.geomorph.2017.09.015, 2017.

644 Spratt, R. M. and Lisiecki, L. E.: A Late Pleistocene sea level stack, *Clim. Past*, 12(4), 1079–1092, doi:10.5194/cp-12-1079-  
645 2016, 2016.

646 Strong, N. and Paola, C.: Fluvial Landscapes and Stratigraphy in a Flume, *Sediment. Rec.*, 4(2), 4–8,  
647 doi:10.2110/sedred.2006.2.4, 2006.

648 Sylvia, D. A. and Galloway, W. E.: Morphology and stratigraphy of the late Quaternary lower Brazos valley: Implications for  
649 paleo-climate, discharge and sediment delivery, *Sediment. Geol.*, 190(1–4), 159–175, doi:10.1016/j.sedgeo.2006.05.023,  
650 2006.

651 Thomas, M. A. and Anderson, J. B.: Sea-Level Controls on the Facies Architecture of the Trinity/Sabine Incised-Valley  
652 System, Texas Continental Shelf, in *Incised-Valley Systems: Origin and Sedimentary Sequences.*, SEPM Society for

653 Sedimentary Geology., 1994.

654 Tofelde, S., Savi, S., Wickert, A. D., Bufe, A. and Schildgen, T. F.: Alluvial channel response to environmental perturbations:  
655 Fill-terrace formation and sediment-signal disruption, *Earth Surf. Dyn.*, 7(2), 609–631, doi:10.5194/esurf-7-609-2019, 2019.

656 Trinity River Authority of Texas: Phase II, Bathymetry and Sediment Collection for Port of Liberty Study., 2017.

657 U.S. Geological Survey: National Water Information System data available on the World Wide Web (USGS Water Data for  
658 the Nation), [online] Available from: <https://waterdata.usgs.gov/usa/nwis/uv?08066500>, 2020a.

659 U.S. Geological Survey: National Water Information System data available on the World Wide Web (USGS Water Data for  
660 the Nation), [online] Available from: [https://waterdata.usgs.gov/nwis/uv?site\\_no=08067000](https://waterdata.usgs.gov/nwis/uv?site_no=08067000), 2020b.

661 Wegmann, K. W. and Pazzaglia, F. J.: Holocene strath terraces, climate change, and active tectonics: The Clearwater River  
662 basin, Olympic Peninsula, Washington State, *Bull. Geol. Soc. Am.*, 114(6), 731–744, doi:10.1130/0016-  
663 7606(2002)114<0731:HSTCCA>2.0.CO;2, 2002.

664 Whipple, K. X.: Implications of sediment-flux-dependent river incision models for landscape evolution, *J. Geophys. Res.*,  
665 107(B2), 2039, doi:10.1029/2000JB000044, 2002.

666 Whipple, K. X., Parker, G., Paola, C. and Mohrig, D.: Channel Dynamics, Sediment Transport, and the Slope of Alluvial Fans:  
667 Experimental Study, *J. Geol.*, 106(6), 677–694, doi:10.1086/516053, 1998.

668 Wickert, A. D. and Schildgen, T. F.: Long-profile evolution of transport-limited, , 17–43, 2019.

669 Wilkerson, G. V. and Parker, G.: Physical Basis for Quasi-Universal Relationships Describing Bankfull Hydraulic Geometry  
670 of Sand-Bed Rivers, *J. Hydraul. Eng.*, 137(7), 739–753, doi:10.1061/(ASCE)HY.1943-7900.0000352, 2011.

671 Womack, W. R. and Schumm, S. A.: Terraces of Douglas Creek, northwestern Colorado: An example of episodic erosion,  
672 *Geology*, 5(2), 72–76, doi:10.1130/0091-7613(1977)5<72:TODCNC>2.0.CO;2, 1977.

673 Young, S. C., Ewing, T., Hamlin, S., Baker, E. and Lupton, D.: Final Report Updating the Hydrogeologic Framework for the  
674 Northern Portion of the Gulf Coast Aquifer, , 283, 2012.

675